VOLUME 114, NUMBER 2
JANUARY 15, 1992

JOURNAL
OF THE
AMERICAN
CHEMICAL
SOCIETY

Angle Selection in EPR and ENDOR Spectra of Rhombic Metal Complexes: Copper Glutamate and Copper [^{15}N]Glutamate Spectra

S. P. Greiner,*,† R. W. Kreilick, and K. A. Kraft‡

Contribution from the Department of Chemistry, University of Rochester, Rochester, New York 14627. *Received March 5, 1991*

Abstract: Nitrogen ENDOR powder patterns have been observed from powdered samples of copper glutamate and isotopically substituted copper glutamate with ^{15}N at approximately 10 K. By irradiating with radio frequency at the highest and lowest ENDOR frequencies and sweeping the field, single-crystal-like ENDOR-induced EPR spectra have also been obtained. Through analysis of these data, the orientations of molecules contributing to each spectrum are readily calculated. The magnitude and relative orientations of the nitrogen hyperfine and quadrupolar tensors with respect to the **g** tensor have been determined through this analysis.

Introduction

Metal complexes containing naturally abundant nitrogen are ubiquitous in nature. Both electron spin resonance (EPR) and electron nuclear double resonance (ENDOR) have been used to determine hyperfine and quadrupolar interactions for nitrogen atoms. The hyperfine and quadrupolar interactions of nitrogen atoms contained in ligands coordinated to metal atoms are often small and cannot be directly resolved in EPR spectra. However, ENDOR spectra often have better resolution and can be used to determine these hyperfine interactions. In amorphous or highly disordered samples of metal complexes, a nitrogen atom with a moderate to large hyperfine interaction may contribute significantly to the line shape of the powder spectrum. The general shape of the powder pattern is determined by selected molecular orientations which fulfill the resonance condition at any given field values. The molecular orientations which are in resonance at any single field value are governed not only by the anisotropy of the **g** and metal hyperfine tensor but by the hyperfine interaction of the nitrogen atom as well. The nitrogen hyperfine interaction may also contribute to the overall ENDOR intensity.

Copper complexes with one or more nitrogen atoms bonded directly to the metal atom usually exhibit a large nitrogen hyperfine interaction. In this paper, we interpret EPR and ENDOR spectra of copper complexes with rhombic **g** tensors and ligands with nitrogen atoms. We also demonstrate how the technique of ENDOR-induced EPR (EI-EPR) can be used to determine the orientation of the hyperfine and g axes systems with respect to the molecular axis system. This paper presents experimental EPR and ENDOR results obtained from an investigation of powdered complexes of copper glutamate and ^{15}N isotopically substituted glutamate, doped into a zinc glutamate host.

Copper glutamate exists in the crystalline state with three glutamate groups plus one water molecule bound to the central copper atom in a highly distorted octahedral configuration.[1] Five oxygen atoms and a single nitrogen atom are coordinated to copper. This molecule serves as an excellent example of a model complex exhibiting rhombic symmetry with a single ligated nitrogen atom. The ^{15}N-substituted species shows only the hyperfine interaction while the ^{14}N complex exhibits both hyperfine and quadrupolar interaction.

Theory

The equation relating the resonant field position in an EPR spectrum to the principal components of the **g** tensor (g_i), the

† Current address: Allied-Signal Inc., 50 East Algonquin Rd., Box 5016, Des Plaines, IL 60017-5016.
‡ Current address: Department of Radiology, Medical College of Virginia, Richmond, VA 23298.

(1) Gramaccioli, C. M.; Marsh, R. E. *Acta Crystallogr.* **1966**, *21*, 594.

0002-7863/92/1514-391$03.00/0

principal components of the hyperfine tensors (A_{ji}), and the angles (θ, φ) of the field vector with respect to the g axis system is given by

$$H = \left[\frac{h\nu_0 - \sum_i A(\theta,\phi)\, m_i}{g(\theta,\phi)\,\beta} \right] \quad (1)$$

with the effective g and A values shown as

$$g(\theta,\phi) = (\sum_i (g_i h_i)^2)^{1/2} \quad (2)$$

$$A(\theta,\phi) = \left(\frac{\sum_i (\sum_j A_{ji} g_j h_j)^2}{g(\theta,\phi)} \right)^{1/2} \quad (3)$$

and direction cosines

$$h_1 = \cos\phi \sin\theta \qquad h_2 = \sin\phi \sin\theta \qquad h_3 = \cos\theta \quad (4)$$

The equation for the frequencies of ENDOR absorption is given by[2,3]

$$\nu(H,m_s) = \left[\sum_{j=1}^{3} \left[\frac{m_s}{g(\theta,\phi)} (\sum_{j=1}^{3} g_j h_j A_{ji}) - h_i \nu_N \right]^2 \right]^{1/2} + (Pm_s/2)(3m_i^2 - I(I+1)) \quad (5)$$

with the nuclear Larmor frequency shown as

$$\nu_N = g_N \beta_N H_0 / h \quad (6)$$

and the quadrupolar term by

$$Pm_s = \frac{\vec{n}|(m_s/g(\theta,\phi))\bar{A}\vec{g} - \nu_N \bar{E}|^T Q |(m_s/g(\theta,\phi))\bar{A}\vec{g} - \nu_N \bar{E}|\vec{n}}{\vec{n}|(m_s/g(\theta,\phi))\bar{A}\vec{g} - \nu_N \bar{E}|^T |(m_s/g(\theta,\phi))\bar{A}\vec{g} - \nu_N \bar{E}|\vec{n}} \quad (7)$$

with

$$\vec{n} = \cos\phi \sin\theta\, \vec{i} + \sin\phi \sin\theta\, \vec{j} + \cos\theta\, \vec{k} \quad (8)$$

The parameters with the arrows overhead indicate vectors, while the overhead bar indicates tensors. The "T" signifies matrix transpose. $\bar{E}$ is the unit tensor in these equations. The ENDOR frequency is dependent on the relative orientation of the external magnetic field with respect to the g axis system through both the hyperfine and quadrupolar terms.

Expanding the numerator in eq 7 yields the following three terms:

$$Pm_s = \left(\frac{m_s}{g} \right)^2 \vec{n}^T \vec{g}^T \bar{A}^T Q \bar{A} \vec{g} \vec{n} - \nu_N \left(\frac{m_s}{g} \right) \vec{n}^T (\vec{g}^T \bar{A}^T Q + Q \bar{A} \vec{g}) \vec{n} + \nu_N^2 \vec{n}^T Q \vec{n} \quad (9)$$

The first term to the left of the equal sign in eq 9 is similar to what has been used previously to measure quadrupolar couplings in ENDOR,[4] and spectral analysis without using the other two terms leads to incorrect evaluation of quadrupolar couplings in some cases.[5] Because the middle term has a linear dependence on the electron spin, adjacent ENDOR resonances can be separated by frequencies different than twice the Zeeman frequency. A $-^1/_2$ electron spin will add that term to the total frequency, while a $+^1/_2$ electron spin will subtract it. Thus, ENDOR analysis must utilize the full expression of eq 7.

The nuclear hyperfine interaction tensor is defined as a sum of two terms: the Fermi contact interaction and the dipolar interaction tensor.[2,3,5-8] The latter is best understood and described by the classical interaction of two magnetic dipoles. Classically, two interacting dipoles separated by some distance R will give the largest interaction energy when they are aligned parallel to one another, along the direction of a vector connecting the two moments. To a first approximation, in a typical X-band EPR experiment the electronic and nuclear moments follow the alignment of the external magnetic field. Only when the field vector is aligned along the direction of a vector connecting the two moments can both moments be aligned parallel and along their connecting vector. One would therefore expect the largest measured hyperfine interaction to occur, strictly on classical grounds, when this is the case. In subsequent discussions, these ideas are presumed.

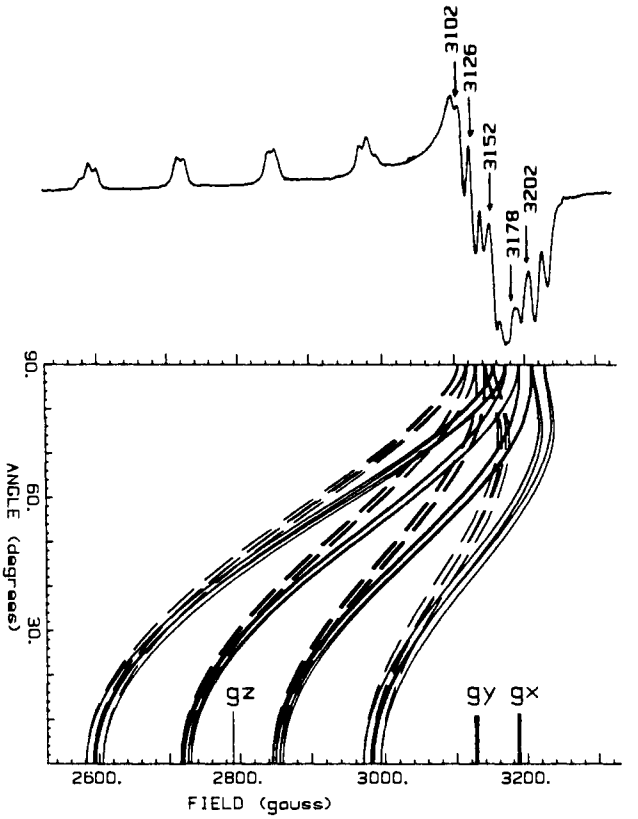

Figure 1. EPR powder pattern of copper [^{15}N]glutamate with a plot of θ versus field beneath it. Dashed curves are for $\varphi = 90°$ and the solid curves for $\varphi = 0°$. The arrows point to the locations ENDOR spectra were acquired. The microwave frequency was 9.128 GHz, and the EPR parameters are listed in Table I.

Experimental Section

(a) Sample Preparation. Stoichiometric weights of CuO and $Zn(OH)_2$ were added to a slurry of excess glutamic acid, and the mixture was stirred for 24 h in D_2O at 60 °C. The light blue precipitate was collected and dried in a drying tube under vacuum overnight. Enough sample was prepared to yield approximately 20 mg of product, a convenient ENDOR sample size. The reactions were assumed to go to completion.[6] To synthesize the copper [^{15}N]glutamate, [^{15}N]glutamic acid (purchased from MSD Isotopes) was substituted in place of normal glutamic acid. Zinc glutamate is isomorphic with copper glutamate and provides a suitable host system for a powdered sample. Typically, the samples were 0.7% copper glutamate in a zinc glutamate host.

(b) Instrumentation. The EPR and ENDOR spectrometer has already been described.[7,8] An IBM PC was used for data acquisition and storage, utilizing a program written with the ASYST programming language. Experimental conditions consisted of frequency modulation at 19 kHz, FM modulation excursion of 30 kHz, temperature near 10 K, and rf power over 100 W while saturating the EPR transition. Microwave power typically was between 0.2 and 4 mW.

Results and Discussion

Copper [^{15}N]Glutamate. (i) EPR and Angular Selection. Figure 1 shows an EPR powder pattern of copper [^{15}N]glutamate. On

(2) Weil, J.; Anderson, J. *J. Chem. Phys.* **1961**, *35*, 1410.
(3) Iwasaki, M. *J. Magn. Reson.* **1974**, *16*, 417.
(4) Brown, T. G.; Hoffman, B. M. *Mol. Phys.* **1980**, *39*, 1073.
(5) Greiner, S. P. Thesis, University of Rochester, 1987.
(6) Kraft, K. A. Thesis, University of Rochester, 1982.
(7) Hurst, G. C.; Henderson, T. A.; Kreilick, R. W. *J. Am. Chem. Soc.* **1985**, *107*, 7294.
(8) Henderson, T. A.; Hurst, G. C.; Kreilick, R. W. *J. Am. Chem. Soc.* **1985**, *107*, 7299.

Table I

			x	*y*	*z*	
g			2.043	2.083	2.339	
Cu hyperfine (MHz)			52	37	410	
N (MHz)	θ (deg)	φ (deg)	cosine angle			
-50.1	78–79	10–18	0.952	0.327	0.190	
-32.85	89–91	100–108	-0.241	-0.970	0.0	
-32.85	10–12	190–198	-0.193	-0.048	0.979	
N (MHz)	θ (deg)	φ (deg)	cosine angle			*Q*
35.80	83	18–26	0.920	0.371	0.121	-1.29
23.49	90	108–116	-0.374	0.927	0.0	1.01
23.48	15–16	198–206	-0.248	-0.100	0.967	0.27

the bottom of the diagram is a θ versus field plot for this spectrum. Both ^{63}Cu and ^{65}Cu were considered by accounting for the percentages of natural abundance of each for the calculation of this graph. The isotope abundance primarily affects the intensity of the EPR spectrum but has an influence on the orientation selection as well.[5] Table I lists the measured EPR and ENDOR parameters determined from EPR, ENDOR, and EI-EPR simulations.[5,9]

Normally, the first-order EPR selection rules ($\Delta M_s = \pm 1$) obviate the detection of quadrupolar splittings in EPR spectra. However, if a quadrupolar interaction in a paramagnetic species is large, it can produce a second-order effect. An unequal spacing of the resonances in the hyperfine pattern of the EPR absorption may then appear. The θ–field curves of Figure 1 (and later Figure 7) are created from experimentally measured parameters of the EPR spectrum, refined through simulation of the spectrum using the first-order equation (1) and are independent of the copper quadrupolar interaction. This is admissible when simulating transition-metal complexes because of the large field excursions and linewidths that the experimental spectra generally have. Errors in the experimental EPR spectra are typically 5 MHz. Neglecting perturbations of this magnitude will not introduce significant errors when comparing simulated versus experimental EPR spectra[9] or alter the orientation selection described by the curves in the bottom of Figure 1.

The paths describing the molecular orientations which contribute to the spectrum are shown on the bottom of this diagram. There are four curves for each isotope of copper, split into doublets by the effect of the ^{15}N hyperfine interaction. The molecule has rhombic symmetry so the EPR spectrum is dependent upon both θ and φ. Sixteen curves are plotted as a function of field for two orientations of the angle φ: 0 and 90°. The 16 curves plotted for φ equal to 0° center around g_x (solid curves) while the other 16 curves (broken curves) center around g_y. Arrows mark the locations where ENDOR spectra were acquired in the EPR spectrum of Figure 1. Five nitrogen ENDOR spectra were obtained at 25-G increments from the EPR spectrum, starting at 3102 G. For each of these field locations the selected orientations which contribute to the ENDOR spectrum can be plotted on a graph of θ versus φ. Figure 2 shows plots of θ versus φ for field values of 3102 and 3202 G.

Figure 2a has 16 curves, four for each isotope of copper where each is split into doublets by the ^{15}N hyperfine interaction. The solid curves represent ^{63}Cu while the dashed curves represent ^{65}Cu. The EPR absorption can be represented as an ellipsoid in which the resonant field is given by a constant-length vector from the origin to the surface of the ellipsoid. Each curve in Figure 2 represents the orientations the field selects as it scribes a path on the first two quadrants of the upper hemisphere. If one assumes that the copper and nitrogen hyperfine axes are coincident with the *g* axis system, then one would place the copper–nitrogen bond on the g_x axis where $\theta = 90°$ and $\varphi = 0°$. When the field vector assumes an orientation parallel to this axis, the maximum ENDOR frequency should occur in the ENDOR spectrum. Figure 2a indicates for ENDOR spectra acquired near 3102 G the field

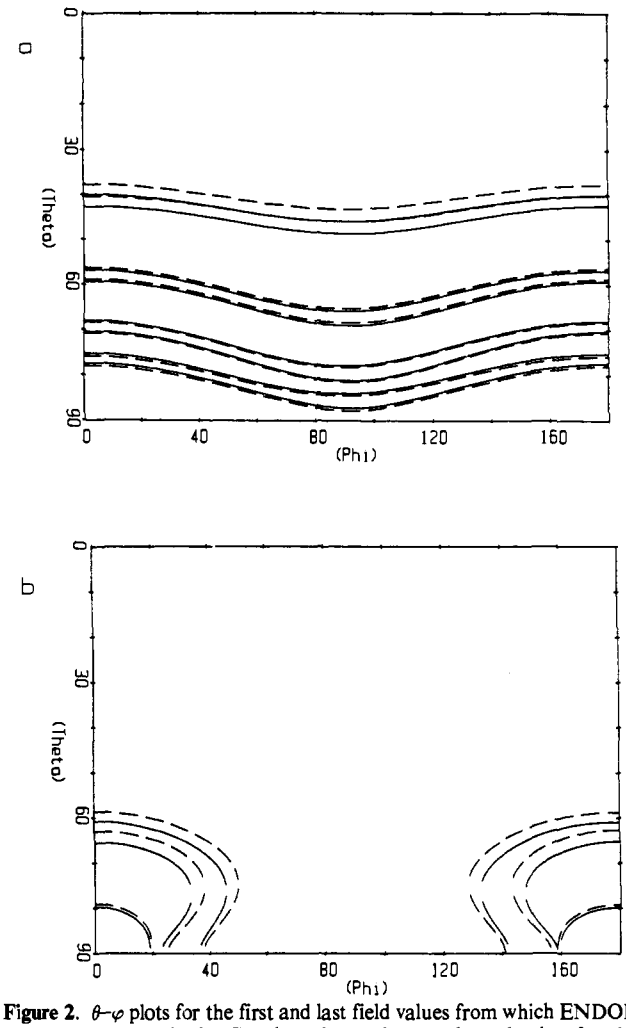

Figure 2. θ–φ plots for the first and last field values from which ENDOR spectra were acquired. Graph a shows the angular selection for the ENDOR spectra acquired at 3102 G while graph b shows the angular selection for 3202 G. Dashed and solid curves differentiate the orientations selected for each isotope of copper (^{63}Cu and ^{65}Cu, respectively).

cannot be aligned along the g_x (copper–nitrogen bond) axis and therefore should not give splittings at the largest ENDOR frequency.

The closest approach of the field vector to the copper–nitrogen bond (Figure 2a) occurs where each curve crosses the g_x–g_z plane ($\varphi = 0°$ for all θ). Sixteen orientations occur when φ assumes a value of 0° for values of θ less than 90°. Each of these orientations should give rise to consecutive ENDOR turning points, shy of the maximum frequency turning points but dependent upon the angle between the Cu–N vector and the field direction. The minimum ENDOR frequency occurs when the field vector is directed perpendicular to the g_x axis. From Figure 2a, all curves passing through a plane at $\varphi = 90°$ for all θ (field confined on the g_y–g_z plane) contribute to low-frequency turning points in the ENDOR spectrum. It is observed from this diagram that all 16 curves have this value of φ at least once.

(ii) ^{15}N ENDOR Spectra. The nitrogen ENDOR spectra of polycrystalline copper [^{15}N]glutamate were acquired at about 10 K. Spectra recorded with a frequency sweep between 15 and 27 MHz are shown in Figure 3. The peak which varies from 16.6 MHz (Figure 3a) to 17.0 MHz (3e) is due to proton and is not discussed here. Figure 4 shows ENDOR spectra acquired at the same field values as those in Figure 3 but obtained with greater sensitivity and sample volume. In these spectra the radio frequency was swept from 21.0 to 27.5 MHz. This expanded sweep excludes the absorption peaks at 15.1 and 17.8 MHz but shows a series of smaller peaks in the high-frequency region.

The ^{15}N ENDOR spectra show four clearly defined peaks marked with arrows in Figure 3a–c. These four peaks are defined

(9) Greiner, S. P.; Baumgarten, M. *J. Magn. Reson.* **1989**, *83*, 630.

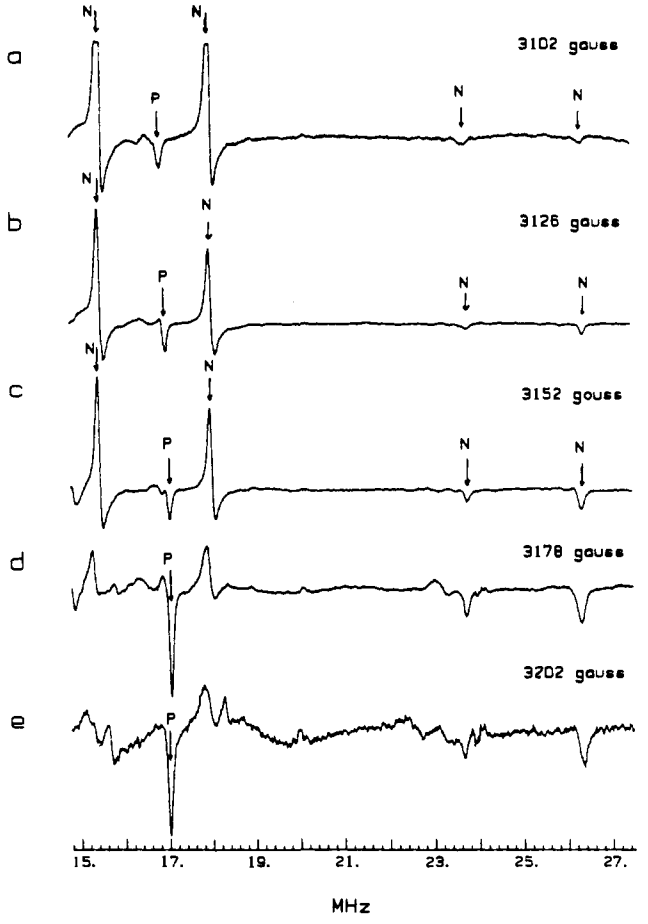

Figure 3. ^{15}N ENDOR spectra of copper [^{15}N]glutamate acquired at the field values indicated. Arrows point to turning point positions of the ENDOR powder pattern. The single arrow around 17 MHz points to a proton resonance. Microwave frequency was 9.128 GHz, and the temperature was 10 K.

Table II. Intermediate Peaks (MHz) of the ^{15}N ENDOR Spectrum

3102 G	3126 G	3152 G	3179 G	3202 G
21.14	21.75	21.84	23.26	22.75
21.56	22.20	22.42	23.90	23.30
21.99	22.50	23.06	25.27	23.90
22.43	22.89	23.44	25.72	25.50
22.90	23.30	23.94		
23.22	23.94	24.98		
23.97	24.29	25.53		
24.93	25.43	25.98		
25.32	25.86			
25.77				

as the high- and low-frequency turning points for the powder patterns observed in the spectra. The peaks of lower intensity between 21.0 and 26.3 MHz are due to 16 orientations where the field vector more closely approaches the copper–nitrogen bond. Table II lists the frequencies of these intermediate peaks. Qualitatively, the ENDOR spectrum can be interpreted as consisting of one powder pattern and two turning points for each value of the electron spin. A more detailed description will be presented in subsequent discussion. The nitrogen ENDOR spectrum from the g-parallel region of the EPR spectrum was also acquired (not shown) and exhibits two peaks at frequencies 15.1 and 17.8 MHz. The ENDOR powder pattern has a very small frequency excursion at this region of the EPR spectrum, because the field vector is confined to a very local region around the g_z axis. Thus, the g-parallel region nitrogen ENDOR resonances are caused by molecules where the field vector is oriented nearly along the g_z axis, along one of the nitrogen hyperfine axes which is orthogonal to the nitrogen–copper bond. This corresponds to one of the

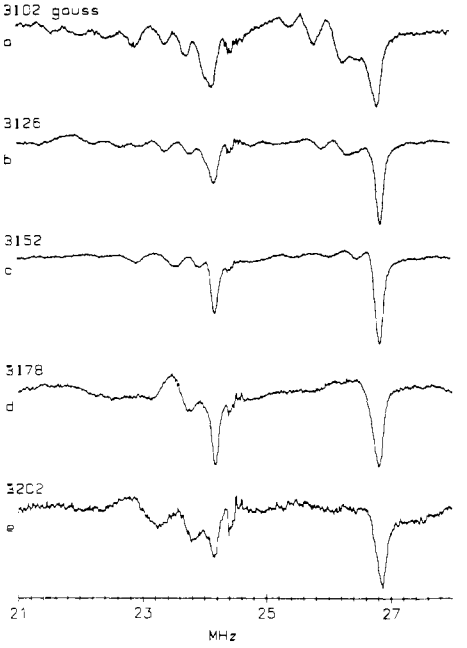

Figure 4. Expanded view of the ENDOR spectra shown in Figure 3, where a larger sample and higher sensitivity were used.

minimum hyperfine axes so that the resonances occur at the lowest possible ENDOR frequency.

In the ENDOR powder pattern spectra of Figure 3a–c two resonances are observed at the same frequency as in the g-parallel spectrum: 15.1 and 17.8 MHz. These are the lowest observed ENDOR resonances occurring when the field is perpendicular to the maximum hyperfine axis, aligned somewhere on the g_y–g_z plane. Thus, when the field is confined along the g_z or g_y axis, the ENDOR resonances are at the same frequency. We conclude from these data that the components of the nitrogen hyperfine tensor perpendicular to Cu–N bond axis have the same value. We define this plane made up of the two identical hyperfine axes nearly along g_y and g_z as "the plane of minimum splitting".

The intensities of the turning points differs for the low- and high-frequency extrema. The major contribution to the intensity difference is due to the populations of the various orientations at any single field value. For instance, 32 orientations may fall on the plane of minimum splitting shown by the curves in the upper hemisphere of Figure 2a ($\varphi = 90°$ for all θ). There are two allowed orientations for each curve (one at φ near 90° and one for φ near 270°). The identical result occurs when you include the four quadrants of the bottom hemisphere (θ varying from 90 to 180° while φ varies from 0 to 360°) due to the symmetry of the **g** and **A** tensors. A single orientation contributes to the high-frequency turning points when the field is parallel or antiparallel to the Cu–N axis. This results in a single intensity ratio of 1:32 for the high- to low-frequency turning points and is about the ratio observed in the ENDOR spectrum of Figure 3a.

In Figure 3d, the low-frequency splittings at 15.1 and 17.8 MHz have much lower intensity as compared to those peaks observed in Figure 3a–c. The reduction in intensity is due to fewer contributing molecular orientation where the field crosses the plane of minimum splitting at the field value of this spectrum. In spectrum e, the resonances at 15.1 and 17.8 MHz have nearly disappeared into the base line.

As the field is increased beyond the position marked by g_y in the EPR spectrum, the field vector is confined to selecting orientations around the g_x axis. This situation is represented in Figure 2b by ellipsoidal curves around the g_x axis. Thus, the curves describing the selected orientations no longer pass through the plane of minimum splitting, and the low-frequency turning points should not be observed. As the field continues to increase, some of the curves at the higher θ values tend to be excluded from contributing to the ENDOR (EPR) resonance. This is a result of certain spin manifold combinations of nitrogen and copper no

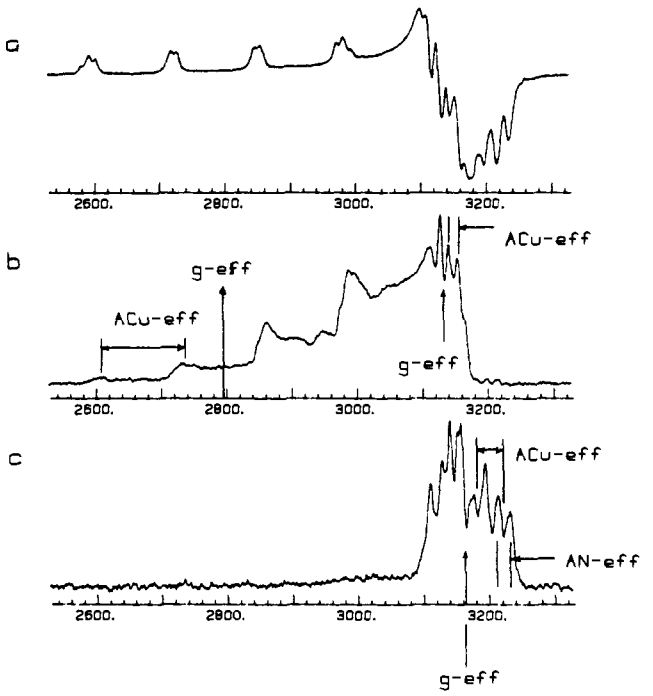

Figure 5. (a) Normal EPR spectrum of copper [^{15}N]glutamate. (b) EI-EPR spectrum with an observing frequency of 15.14 MHz and g_{eff} = 2.33 and A_{eff}(Cu) 410 MHz at lower field while at higher field g_{eff} = 2.084 and A_{eff}(Cu) = 42 MHz. (c) EI-EPR spectrum with an observing frequency of 26.4 MHz, g_{eff} = 2.058, A_{eff}(Cu) = 102 MHz, and $A_{N(eff)}$ = 51 MHz. The microwave frequency was 9.127 GHz for all spectra.

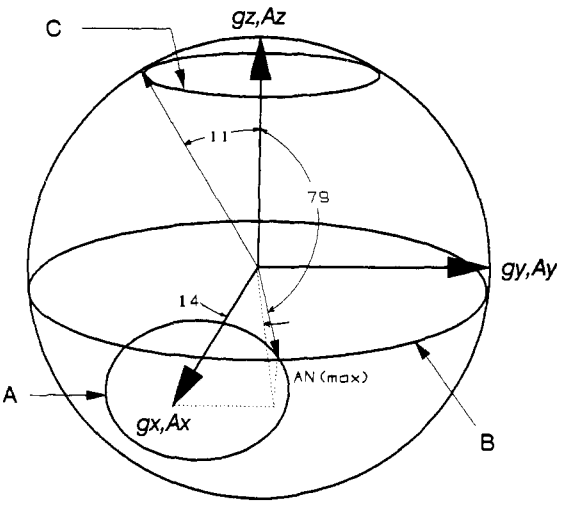

Figure 6. Solutions to eqs 2 and 3 drawn on a unit sphere for constant g_{eff} = 2.058 (curve A) and A_{eff}(Cu) = 102 MHz (curve B) as measured from the EI-EPR spectra (see text). At the top are also shown the solutions to eqs 2 and 3 (curve C) for the lower field region of the EI-EPR spectrum in Figure 5b. The solutions of eqs 2 and 3 for the region at higher field of Figure 5b are omitted for clarity but resemble curves A and B where the constant g_{eff} curve has the form of B and the constant A_{eff}(Cu) curve has the form of A but now surrounds the gy axis.

longer satisfying the resonance condition of eq 1, and thus in Figure 2b fewer curves are observed than in Figure 2a. As the field continues to select orientations around the g_x axis and as the number of allowed spin manifold combinations decreases, fewer and fewer curves pass through the plane of minimum splitting and the intensity of the low-frequency turning point decreases. By comparing the signal intensity of the low-frequency turning points in the ENDOR spectra of Figure 3a–d, one observes the effect of orientation on the intensity of ENDOR spectra.

Assuming the nitrogen hyperfine axis system is collinear with the copper hyperfine and g axis systems, one predicts that the high-frequency peaks in the ENDOR spectrum result when the field vector is aligned along the Cu–N bond (the g_x axis). In Figure 2a this corresponds to $\theta = 90°$ and $\varphi = 0°$. There are no allowed orientations with those values of θ and φ for this field value. This result shows that the Cu–N bond cannot be along the g_x axis. In order to analyze correctly the ENDOR spectra, one must determine the angle between the Cu–N bond axis and the g_x axis by either single-crystal ENDOR or EI-EPR.

(iii) ENDOR-Induced EPR. Figure 5 exhibits three spectra: an EPR spectrum and two EI-EPR spectra. The EI-EPR spectra were obtained by keeping the irradiating frequency constant while sweeping the field. The top spectrum is the normal first-derivative EPR spectrum. The middle spectrum was acquired with the radio frequency set at 15.14 MHz, corresponding to one of the low-frequency turning points in the normal ^{15}N ENDOR spectrum. The bottom spectrum was acquired with the radio frequency centered at 26.4 MHz. All three spectra are shown with the same field width and were acquired with a microwave frequency of 9.127 GHz.

The EI-EPR spectrum acquired with the irradiating frequency at 15.14 MHz is identical to a two-dimensional EPR powder pattern. Only those molecules which lie on a plane defined by the two axes of the minimum nitrogen hyperfine tensor exhibit an ENDOR frequency at 15.14 MHz. Thus, only molecules on this plane are observed in the EI-EPR spectrum. The frequency where the maximum resonance occurs in the ENDOR spectrum is 26.4 MHz. This ENDOR frequency will occur for molecules where the orientation of the field vector is along the copper–nitrogen bond. The EI-EPR spectrum on the bottom of Figure 5 was acquired with the irradiating frequency at 26.4 MHz and is nearly a single-crystal EPR spectrum. Only molecules that have the field vector aligned along their copper–nitrogen bond (maximum nitrogen hyperfine axis) contribute to the EI-EPR spectrum.

To analyze the EI-EPR spectra, we made use of the known EPR parameters from previous measurements (the values of g_x, g_y, g_z, A_x(Cu), A_y(Cu), and A_z(Cu) listed in Table I) and the effective g and copper hyperfine values measured from the EI-EPR spectrum (these are given in the caption of Figure 5). Values of θ and φ giving the rotation of the nitrogen hyperfine axes from the g axes may be found through simultaneous solution of eqs 2 and 3. A graphical solution may also be found by iterative solutions of 2 and 3 to determine θ,φ pairs.

For the EI-EPR spectrum with the observer frequency at 26.4 MHz, the single-crystal EPR spectrum, the solutions of eq 2 for θ and φ describe a curve of constant g (equal to 2.058) drawn around the g_x axis as shown in Figure 6. The solutions from eq 3 describe a curve of constant A_{eff} (equal to 102 MHz) drawn around the g_z axis. The only orientations which are simultaneous solutions to eqs 2 and 3 are those orientations at the positions the curves overlap. This EI-EPR spectrum is caused only from molecules that have the field vector aligned along their copper–nitrogen bond. Thus, the position of overlap must define the direction of the copper–nitrogen bond, and the values of θ and φ at the overlap position define the coordinates of the maximum hyperfine axis for nitrogen. These coordinates are between 78 or 79° for θ_n and between 10 and 18° for φ_n. The same result is obtained by analytical solution of the simultaneous equations.

A similar analysis for the middle spectrum of Figure 5 yields a value of approximately 11° in θ_n. The solutions to eqs 2 and 3 for this spectrum define equivalent orientations. That is, the curves representing the solutions are approximately superimposed. There are no unique points of overlap for these curves, and φ_n is left undetermined. Figure 6 depicts this situation for the curves surrounding the g_z axis near the top of the diagram. Assuming the three axes of the nitrogen hyperfine tensor are orthogonal and knowing the direction of the maximum hyperfine axis in the g axis system and the angle θ_n as measured from the g_z axis for one of the minimum axes, all three hyperfine axes directions can be determined by simple algebra. The bottom of Table I lists the three axes in the g axis coordinate system which diagonalize the nitrogen hyperfine tensor. The largest hyperfine axis, A_1, points in the direction of the copper–nitrogen bond. Figure 6 depicts this axis.

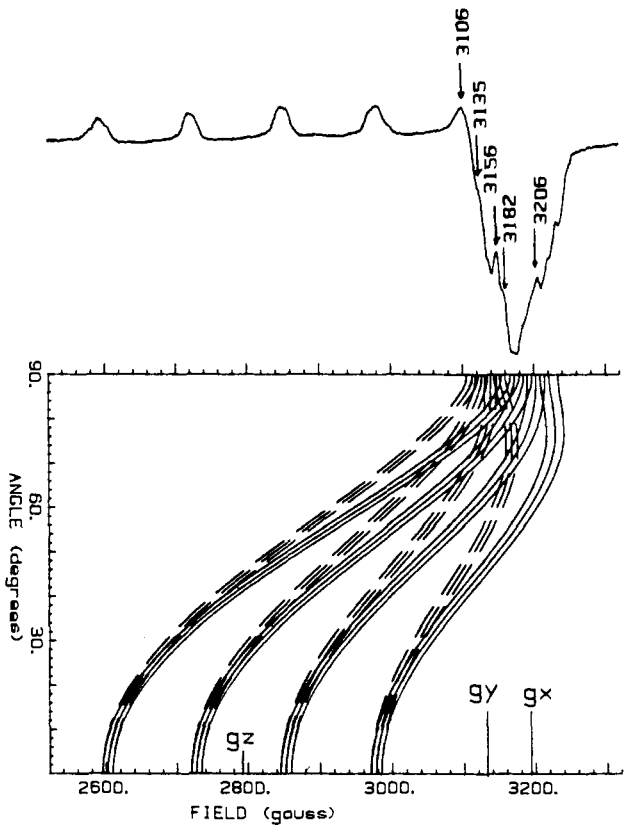

Figure 7. EPR powder pattern of copper glutamate with a plot of θ versus field beneath it for a single isotope of copper. Dashed curves are for $\varphi = 90°$ and the solid curves for $\varphi = 0°$. The arrows point to the locations ENDOR spectra were acquired. The microwave frequency was 9.146 GHz, and the EPR parameters are listed in Table I.

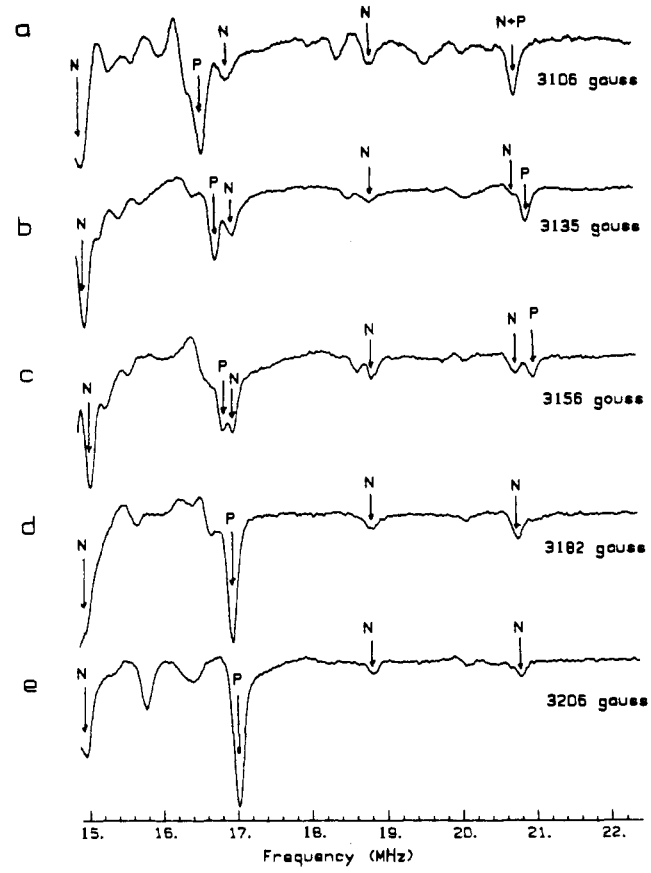

Figure 8. ^{14}N ENDOR spectra of copper glutamate acquired at the field values indicated. Arrows labeled "N" point to high-frequency turning point positions of the ENDOR powder pattern. The single arrow around 17 MHz points to a proton resonance. The microwave frequency was 9.146 GHz, and the temperature was 10 K.

The EI-EPR response is equivalent to an EPR absorption; in fact, it is an EPR response. Thus, the copper quadrupolar interaction plays no part (to first order) in the selection rules for absorption as reported earlier for the EPR analysis and has no impact on the simultaneous solutions to eqs 2 and 3 in this analysis. This would not be true when second-order effects are observed in the EPR spectrum however.

A caveat should be briefly mentioned. The precise direction of the nitrogen hyperfine axes cannot be determined because of the symmetry of the g and A tensors. Thus, four unique solutions to eqs 2 and 3 are found (four points of overlap occur between the curves of constant g and A). For the A_1 axis, φ_n could equally as well have the value 342 to 350° with θ_n = 78–79° or 101–102°. There are four positions the hyperfine axis A_1 could be directed along. Accordingly, A_2 and A_3 could have four positions also. Varying the angle of rotation for the nitrogen hyperfine axis system has almost no effect on the θ versus φ curves of Figure 2. Hyperfine tensor rotation does not cause a noticeable difference in the molecular orientations calculated from EPR spectral parameters. This is because orientation selection is largely determined by the copper hyperfine and g tensors magnitude and orientation and is almost independent of the small ligand hyperfine interaction.

Figure 2a shows that there are orientations contributing to the ENDOR spectra at the maximum hyperfine axis. Values of θ near 79° and φ between 10 and 18° are selected by the field. Thus, there are resonances in the ENDOR spectra centered at $A_{1(max)}/2$. These are the resonances occurring at the frequencies 23.6 and 26.3 MHz in all the spectra of Figures 3 and 4.

Copper [^{14}N]Glutamate. (i) EPR and Angular Selection. Figure 7 contains a plot of the EPR powder pattern of copper glutamate (top) and a graph of θ versus field (bottom). The powder pattern for this complex is similar to that of the ^{15}N species shown in Figure 1. Differences between the two powder patterns result from the magnitude of the nitrogen hyperfine tensor being smaller for ^{14}N then for ^{15}N because of the difference in nuclear g values. The apparent EPR linewidth is larger for the ^{14}N spectrum than for the ^{15}N spectrum. This increase is due to ^{14}N having a nuclear spin of 1, which results in more orientations contributing to the EPR spectrum at any one field value.

The dashed curves of θ versus field graphed on the bottom of Figure 7 show the dependence of the resonance field on the field vectors inclination angle as the vector inclines along the g_y–g_z plane ($\varphi = 90°$). The solid curves show this dependency for the field vector reclining in the g_x–g_y plane ($\varphi = 0°$). There are a total of 24 curves in this diagram, 12 for each of the two values of φ. There are 24 additional curves due to the other isotope of copper, but these have been omitted to make the diagram easier to read. The curves for these two values of φ, 0 and 90°, represent the extrema for the resonant field's dependence on φ. A curve calculated for any other φ value will fall between these two sets of curves.

The EPR powder pattern in Figure 7 includes five arrows at field values of 3106, 3135, 3156, 3182, and 3206 G, indicating where nitrogen ENDOR spectra were acquired. We selected field values near the g_x and g_y positions, as one finds the most interesting orientation selection at these field values.

(ii) ^{14}N ENDOR Spectra. Analysis of nitrogen ENDOR for the copper [^{14}N]glutamate complex is complicated by overlap of the proton and nitrogen resonances. To minimize problems associated with analysis of overlapped lines, we selected peaks in the outer edges of the spectra where the overlap is not as severe.

Figure 8 depicts the high-frequency (15–22 MHz) region of the ENDOR spectra acquired from the five field locations for the ^{14}N complex. There is a proton peak whose position increases with field in these spectra (16.6 MHz at 8a to 17.0 MHz at 8e). This peak is observed in the ENDOR spectrum of the [^{15}N]-glutamate complex also (Figure 3). This proton signal overlaps with a nitrogen resonance at 16.92 MHz; however, the nitrogen signal is nearly independent of field and maintains almost a

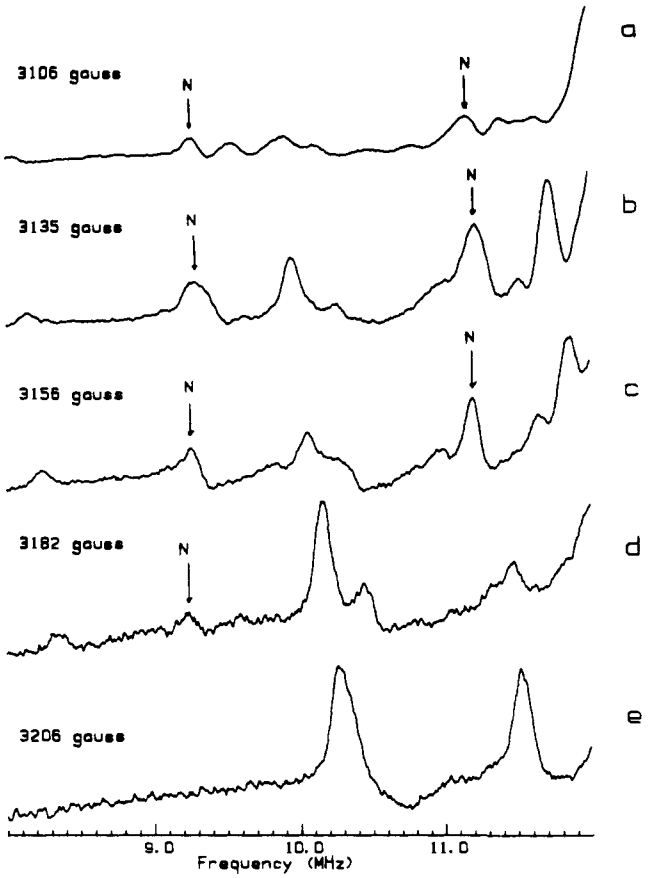

Figure 9. Low-frequency region of the ^{14}N ENDOR spectra. The arrows point to two of the low-frequency nitrogen turning points; the other two turning points are at higher frequency and are obscured by more intense proton resonances.

constant position as the field is increased.

Another proton peak is overlapped with a nitrogen resonance at 20.8 MHz in the ENDOR spectrum of 8a. In 8b the proton resonance has moved up a little to 20.94 MHz (the nitrogen peak at 20.8 MHz is observed as the shoulder on the left of this resonance). Finally, in spectrum 8c the proton signal is observed at 21.014 MHz, and in the spectra acquired at higher fields (8d and e) it has vanished completely. This peak was previously reported by Kraft,[6] and the mirror image of this peak, at around 5.9 MHz, is shown in his thesis.

The high-frequency turning points of these ENDOR spectra are easily observed. Four peaks occur for these turning points due to the effect of the ^{14}N quadrupole moment. For the spectrum shown on Figure 8a, the four peaks are at frequencies of 14.99, 16.92, 18.85, and 20.8 MHz. These high-frequency turning points occur for orientations of the field nearly along the copper–nitrogen bond. These four peaks are observed in all five ENDOR spectra, becuase at least one orientation is selected in each spectrum where the field vector is aligned along the copper–nitrogen bond. Figure 9 contains the low-frequency region (8–12 MHz) of the five ENDOR spectra shown in Figure 8. These spectra show two of the lower frequency turning point resonances (at 9.25 and 11.20 MHz) resulting from the ENDOR powder pattern. The other two peaks occur at higher frequencies and are obscured by the proton resonances. The nitrogen resonances are marked to differentiate them from proton signals.

Analysis of the ENDOR turning point frequencies yields approximate values for the components of the quadrupolar coupling tensor. The separation between adjacent resonances resulting from the same orientation of the field vector is approximately 2 times the nuclear Zeeman frequency or 3 times the quadrupolar coupling (to first order[5]). In order to evaluate these spectra more accurately, ENDOR simulation techniques were performed using the complete equations for the quadrupolar interaction.[5,9] Spectral simulation analysis resulted in refined hyperfine and quadrupolar coupling parameters. The data obtained from this study are contained in Table I.

The ^{14}N ENDOR resonances at the high-frequency turning point region clearly show deviation from 2 times the nitrogen Larmor frequency and 3 times the quadrupolar coupling. For example, the four resonances in 8b are at 14.95, 16.95, 18.79, and 20.7 MHz. The first two peaks are separated by 2.0 MHz while twice the Zeeman splitting is 1.93 MHz, a difference of 70 kHz. The measured frequency errors are approximately one-third the linewidth (30 kHz), so this deviation is large compared to experimental error. In the same spectrum, the second and fourth peaks are separated by 3.75 MHz, while 3 times the Q_z quadrupolar coupling is 3.87 MHz, a difference of 120 kHz. These differences in line separation from 3 times Q_z and the deviation from 2 times the Zeeman splitting are both predicted from the complete equations for the quadrupolar interaction.[5,9] These effects cannot be explained by the simpler equations which are often used to analyze quadrupolar splittings, and this type of analysis leads to incorrect results.[5]

Nitrogen ENDOR spectra acquired from the g-parallel region of the EPR spectrum differed in frequency by only a small amount from the low-frequency turning point resonances in Figure 9. The differences in the resonant frequencies for these ENDOR spectra are due to the difference in the nuclear quadrupolar interaction along the g_y and g_z axes. After accounting for the difference in quadrupolar terms, two of the nitrogen hyperfine axes have been found to be equivalent. This is similar to the results for the [^{15}N]glutamate complex. We conclude from these data that the turning point resonances from Figure 9 result from orientations of the field vector aligned along the plane of minimum splitting.

The additional turning points found in the intermediate-frequency region of the ENDOR spectra of the ^{15}N complex were the result of molecules having the field vector directed between the maximum and minimum hyperfine axes. The ^{14}N ENDOR spectra of Figure 8 also exhibit peaks at intermediate-frequency values between the four turning point resonances. Their origin is identical.

(iii) ENDOR-Induced EPR. The geometry and symmetry of the glutamate complex should be independent of the nitrogen isotope. If this is the case, the hyperfine axis system of the [^{15}N]glutamate complex should be identical to that of the ^{14}N complex.

The principal axes found from the analysis of ENDOR-induced EPR spectra of the ^{14}N and ^{15}N complexes may differ as the quadrupolar interaction affects the EI-EPR spectrum of the ^{14}N complex. The orientation of the nitrogen quadrupolar axes system may differ from the hyperfine axis, and this difference must be accounted for in the analysis of the EI-EPR spectra.

Figure 10 shows two EI-EPR spectra acquired by monitoring the high-frequency extremum of the ENDOR spectra. The radio frequency was held at 21.014 MHz for the top spectrum and 20.04 MHz for the bottom spectrum. The monitoring peak from the upper spectrum is the proton peak mentioned earlier at 21.014 MHz. The proton position cannot be determined accurately because the dipolar approximation loses validity when the hyperfine interaction is large.[5,7,8] However, the EI-EPR spectra indicate that this proton lies close to the x–y plane.

The top EI-EPR spectrum shows a poorly resolved broad peak with an effective g value of 2.075. We are unable to measure individual lines in this broad resonance. The monitoring frequency was held at the largest ENDOR frequency excursion for this proton; thus, the field vector is aligned along the copper–proton vector. The proton must lie on a path of constant g equal to 2.075.

At the higher field values of the lower spectrum are the eight lines indicative of the EI-EPR spectrum from a spin 1 nucleus. Only eight of the twelve are observed because only EPR transitions coupled by the two NMR levels being monitored give the EI-EPR response. The eight peaks are resonances from molecules where the field vector assumes an orientation which results in the highest frequency excursion attainable in the ENDOR spectrum of the ^{14}N atom. The field vector is not oriented along the maximum

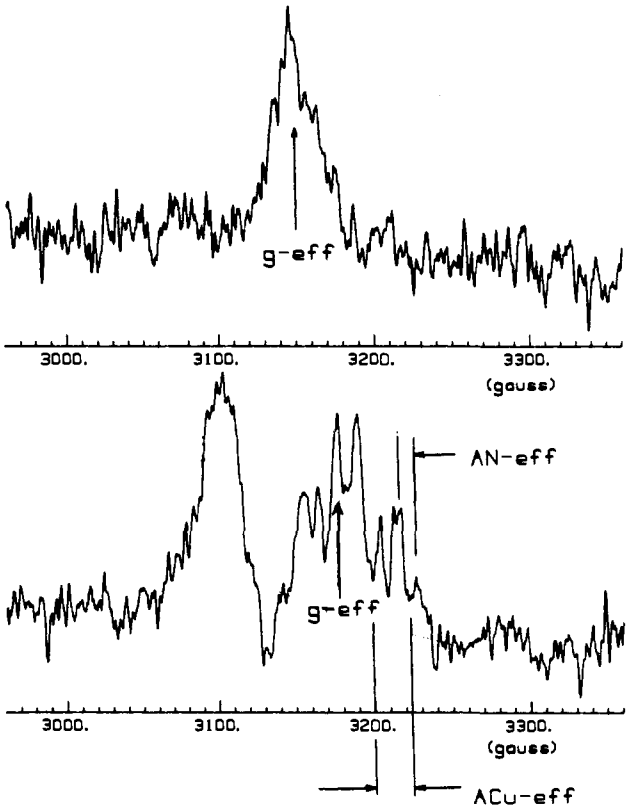

Figure 10. Two EI-EPR spectra collected for the copper glutamate complex. The top spectrum was acquired with an EI-EPR observing frequency of 21.014 MHz, and g_{eff} is 2.075. The lower spectrum has an observing frequency of 20.70 MHz. To the right of the lower spectrum are the eight EI-EPR resonances due to using the ^{14}N ENDOR resonance at 20.7 MHz as the observer, g_{eff} = 2.054, $A_{eff}(Cu)$ = 71 MHz, and $A_{N(eff)}$ = 38 MHz. The microwave frequency was 9.134 GHz for all spectra.

hyperfine axis of the nitrogen hyperfine tensor though, but along some direction where the hyperfine and quadrupolar axes yield the maximum ENDOR frequency. This direction should be some combination of the maximum hyperfine and quadrupolar axes.

To analyze the nitrogen EI-EPR spectrum, the effective g value had to be measured. The eight lines in the right of Figure 10 are centered around a field value of 3183 G. Because the real g value would be centered around a 12-line EPR spectrum, one must make a correction to this field to find the center of the resonance (the center of the fictitious 12-line spectrum). The equation for the effective g value is then given by[10]

$$g_{eff} = \frac{\nu h}{\beta(H_{eff} - A_{N(eff)}/2)} \qquad (10)$$

where H_{eff} = 3183 G and $A_{N(eff)}$ = 38 MHz.

In this equation ν is the microwave frequency, β is the Bohr magneton, h is Planck's constant, H_{eff} is the field at the center of resonance, and $A_{N(eff)}$ is the separation between pairs of peaks in the EI-EPR spectrum. The solution of eq 10 is dependent upon the sign of the hyperfine interaction of nitrogen and upon whether the 0 to 1 or −1 to 0 nitrogen ENDOR transition is the observer. One can calculate a pair of g values from this equation, one equal to 2.055 (positive A, −1 to 0) while the other is equal to 2.044 (negative A, 0 to 1) by subtracting or adding the hyperfine value in the denominator. Since the hyperfine components of ^{14}N coordinate to copper are known to be positive,[11,12] the effective g value is 2.055. We can verify the solution for g because no change is expected in the orientation of the nitrogen hyperfine axis system upon exchange of the isotope of nitrogen. The effective g value from the EI-EPR spectrum of the complex with ^{15}N had a value of 2.058 which is within experimental error of the value from the ^{14}N complex. The nitrogen hyperfine splitting measured from these figures is in accord with the measured maximum hyperfine splitting from the ENDOR spectra. This value of 38 (±4) MHz is within experimental error of the value of 35.8 MHz determined from the ENDOR data.

The large error in the measurement of the hyperfine splitting (±4 MHz) is a result of a slight powder pattern that occurs in the EI-EPR spectrum of the ^{14}N atom. Each spin manifold that contributes to the spectrum is described by a different path on an ellipsoid of allowed orientations.[5] Each curve selects a slightly different set of orientations, and this results in varying linewidths and positions in the EI-EPR spectrum from what one would normally observe in a single-crystal EPR experiment. Thus, the resultant hyperfine parameters measured from the EI-EPR spectra have fairly large errors.

After the simultaneous equations derived from eqs 2 and 3 were solved, the approximate direction vector responsible for the maximum ENDOR frequency for nitrogen was found. The coordinates of this vector are θ_n equal to 83° and φ_n equal to 22° (±4). These coordinates are close to the coordinates describing the direction of the maximum hyperfine axes for ^{15}N. Table I displays the data for the direction of the maximum hyperfine tensor for ^{15}N and ^{14}N. The angular difference between the maximum hyperfine axis for ^{15}N and the direction which gives the maximum ENDOR resonance for ^{14}N is 4° in θ and approximately 8° in φ. The ^{14}N data are only slightly different from the ^{15}N data, resulting in the conclusion that the hyperfine and quadrupolar axis for ^{14}N are almost coincident.

The effective hyperfine values of copper measured from the near single-crystal EI-EPR spectra for the two isotopes of nitrogen are different. The ^{14}N complex has a value of 71 MHz, and the ^{15}N complex has the value of 102 MHz while the field vector direction differs by about 4° (83° for ^{14}N and 79° for ^{15}N) in θ. The discrepancy in the measured copper hyperfine splittings is 31 MHz over these 4° (102–71 MHz). This is easily accounted for by the anisotropy in the copper hyperfine interaction (the energy difference between the three hyperfine axes), where the A_z(Cu) hyperfine splitting is 410 MHz compared to the A_x(Cu) and A_y(Cu) hyperfine splittings of 52 and 37 MHz, respectively.

In Figure 5c, the EI-EPR spectrum of the ^{15}N species had the field vector aligned along the maximum hyperfine axis for nitrogen. While in the spectrum for the ^{14}N species, the field is aligned along a vector sum of the maximum hyperfine and quadrupolar direction vectors. With the addition of the quadrupolar interaction the field vector selects orientations around a direction which gives the maximum ENDOR frequency, rather than a direction of which the hyperfine interaction is at a maximum. This direction is different from the maximum hyperfine axis direction and may be vindicated by the difference in the effective g values (2.058–2.055) for the two spectra. We cannot conclusively determine the direction of the maximum quadrupolar axis (−1.29 MHz) from these data; we can only state it is not coincident with the hyperfine axis and note it is not an unusual result.[13]

Figure 11 depicts the first coordination sphere of copper in the glutamate complex derived from crystal structure data. The origin of the g axis system is centered at the copper atom. The dashed lines point into the plane of the diagram, and the thick solid line points out of the plane of the diagram.

One would intuitively place the four equatorial atoms, N, O_1, O_3, and O_5 in the g_x–g_y plane. Then, the g_z axis would be aligned along the copper–O_2 bond asymmetric between the O_4 and O_2 atoms of Figure 11. In this configuration, the copper–nitrogen bond would be along the g_x axis. This model must be incorrect, however, because the data from the EI-EPR and ENDOR spectra indicate that the maximum hyperfine axis for nitrogen makes an angle of about 17° with the g_x axis. If the g_z axis is equidistant

(10) Niklas, J. R.; Spaeth, J. M. *Phys. Stat. Sol. (b)* **1980**, *101*, 221.
(11) Monoharan, P. T.; Rogers, J. *Electron Spin Resonance of Metal Complexes*; Yen, T. F., Ed.; Plenum Press: New York, 1969.
(12) Maki, A. H.; McGarvey, B. R. *J. Chem. Phys.* **1958**, *29*, 31.
(13) Calvo, R.; Oseroff, S. B.; Abache, C. *J. Chem. Phys.* **1980**, *72*, 760.

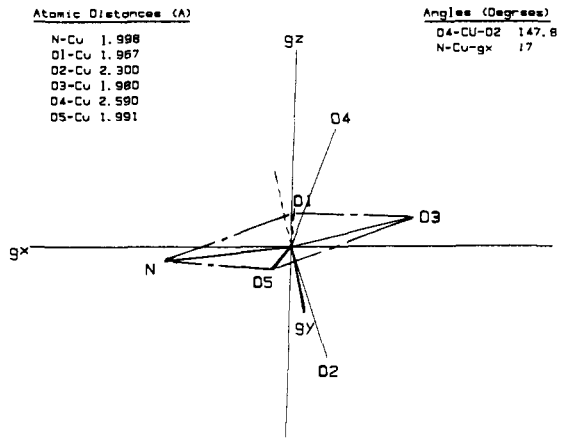

Figure 11. Coordination sphere of copper glutamate with the origin of the g axis system centered at copper. The solid lines are on the plane of the paper. The dashed lines point into the plane of the diagram while the thick, solid lines point out of the plane.

from the Cu–O_2 and Cu–O_4 vectors, the plane formed by the N, O_1, O_3, and O_5 atoms is 17° from the g_x–g_y plane.

Figure 11 depicts this orientation of the g axis system with respect to atom positions. The O_4, Cu, and O_2 atoms make an angle of 148° in the copper glutamate molecule. Each of the "axial" oxygen atoms is 16° from the g_z axis in this structure. The axial oxygens are magnetically equivalent in this picture, which is apparently favored over a structure in which one oxygen would be forced to lie along the g_z axis. The N, O_1, O_3, and O_5 atoms form nearly a square with the O_5 near the positive g_y axis and O_1 near the negative g_y axis. The nitrogen atom lies near the positive g_x axis while O_3 lies near the negative g_x. The magnetic nonequivalency of the x and y axes is probably due to this arrangement of atoms. Our experimental data are completely in accord with this structure.

Conclusions

ENDOR and EI-EPR investigations of ^{14}N and ^{15}N copper glutamate have been conducted to determine hyperfine coupling constants, quadrupolar coupling constants, powder pattern intensity effects, and the relative orientation of magnetic axes. This paper demonstrates that one can select paths of angles by setting the EPR field to a fixed value in the EPR powder pattern. Subsequent analysis of ENDOR spectra requires calculations of all the angles selected by the given field including the affects of nearest-neighbor nitrogen atoms. Low-intensity nitrogen ENDOR transitions, usually ignored in ENDOR studies, require a complete analysis and are accounted for here. This study also shows evidence that the complete equation for the quadrupolar interaction must be used to analyze experimental data correctly. The ENDOR spectra of these compounds indicated that the nitrogen did not lie on one of the principal g axes, which is the usual assumption. EI-EPR was utilized to determine the direction of the nitrogen hyperfine axis system with respect to the g axis system; however, this direction is only consistent with the analysis as there is no unique solution. Knowledge of the relative directions of the hyperfine and g axes allows one to determine the orientation of the g axis system with respect to atomic coordinates.

Acknowledgment. This work was supported by National Institutes of Health Grant GM-22793. We express our appreciation to Dr. Thomas Henderson for many helpful discussions and Dr. David Rowlands for writing the spectrometer acquisition software.

Registry No. Copper glutamate, 36015-31-3.

The Phenylcyclooctatetraene Anion Radical and Dianion: An Intramolecular Charge and Spin Distribution Isotope Effect

Gerald R. Stevenson,* Richard D. Burton, and Richard C. Reiter

Contribution from the Department of Chemistry, Illinois State University, Normal, Illinois 61761. *Received March 18, 1991*

Abstract: EPR studies on the anion radicals and ^{13}C NMR studies of the dianions of phenylcyclooctatetraene ([6]–[8]), phenylcyclooctatetraene-d_7, and phenyl-d_5-cyclooctatetraene show that deuteriation of the cyclooctatetraenyl moiety perturbs and phenyl group spin and charge distributions in the anion radical and dianion, respectively. However, deuteriation of the phenyl moiety does not alter these distributions in the cyclooctatetraenyl moiety. The upfield shift in the chemical shifts of the phenyl carbons in the dianion and the increased spin density in the phenyl moiety in the anion radical, resulting from deuteriation of the eight-membered ring, is explained in terms of the different degrees of twist between the COT and phenyl rings. Since there is more zero-point energy in the coplanar arrangement and the force constant for C–D or C–H stretching mode should be maximized in a coplanar arrangement, [6]–[8]$^{\bullet-}$ will tend to be more twisted than will [6]–[8]-$d_7^{\bullet-}$. The deuteriation studies have further shown that the nature of the spin distribution in the anion radical of [6]–[8] has long been fundamentally misunderstood.

A quarter of a century ago the anion radical of phenylcyclooctatetrane ([6]–[8]$^{\bullet-}$) was reported for the first time.[1] The spin distribution in this system is of particular interest since [6]–[8] is the only existing molecular system where aromatic and antiaromatic (in the Hückel sense) annulenes ([6]annulene and [8]annulene) are directly interconnected. Consequently, the spin and charge distributions in [6]–[8]$^{\bullet-}$ have been the subject of numerous reports.[2] In 1974 Rieke and Copenhafer[2a] obtained an EPR spectrum of this anion with unprecedented resolution via the Li reduction of [6]–[8] in an HMPA–DME solvent mixture.

(1) Carrington, A.; Moss, R. E.; Todd, P. E. *Mol. Phys.* **1966**, *12*, 95.

(2) (a) Rieke, R. D.; Copenhafer, R. A. *Electroanal. Chem. Interfacial Electrochem.* **1974**, *56*, 409. (b) Stevenson, G. R.; Echegoyen, L. *J. Am. Chem. Soc.* **1974**, *96*, 5452. (c) Stevenson, G. R.; Echegoyen, L. *J. Phys. Chem.* **1975**, *79*, 929. (d) Alegria, A.; Diaz, N.; Echegoyen, L.; Maldonado, R.; Colon, J. T. *J. Org. Chem.* **1982**, *47*, 5386. (e) Stevenson, G. R.; Forch, B. E. *J. Phys. Chem.* **1981**, *85*, 378. (f) Stevenson, G. R.; Echegoyen, L. *J. Am. Chem. Soc.* **1986**, *108*, 5509. (g) Echegoyen, L.; Nieves, J.; Maldonado, R.; Alegria, A.; Stevenson, G. R.; Reiter, R. C.; Clark, G. *J. Phys. Chem.* **1986**, *90*, 1241.

0002-7863/92/1514-399$03.00/0